Nonlinear Optics (WiSe 2017/18)
Lecture 8: November 14, 2017

Chapter 5: The electro-optic effect and modulators

5.1 The linear electro-optic effect

5.1.1 Longitudinal electro-optic effect and modulators

5.1.2 Transverse electro-optic effect and modulator

5.2 Electro-optic amplitude modulator

5.3 Electro-optic phase modulator

5.4 Microwave modulator

→ Boyd

In an arbitrary coordinate system we can express the index ellipsoid (sometimes also called optical indicatrix) or the inverse dielectric susceptibility tensor as quadratic form $(1/n^2)_i$ connected to dielectric permeability tensor ε_{ij}

$$\left(\frac{1}{n^2}\right)_1 x^2 + \left(\frac{1}{n^2}\right)_2 y^2 + \left(\frac{1}{n^2}\right)_3 z^2 + 2\left(\frac{1}{n^2}\right)_4 yz + 2\left(\frac{1}{n^2}\right)_5 xz + 2\left(\frac{1}{n^2}\right)_6 xy = 1,$$
$$(5.1)$$

introducing the contracted notation using 1-6. If the coordinate system coincides with the principle-axis system of the index ellipsoid, the mixed terms vanish. For the case of the linear electro-optic effect, an applied electric field leads to a deformation of the index ellipsoid according to

$$\Delta\left(\frac{1}{n^2}\right)_i = \sum_{j=1}^{3} r_{ij} E_j,$$
$$(5.2)$$

with $E_1 = E_x$, $E_2 = E_y$, $E_3 = E_z$. It thus follows, e.g.,

$$\Delta\left(\frac{1}{n^2}\right)_1 = r_{11} E_x + r_{12} E_y + r_{13} E_z,$$
$$(5.3)$$

or

$$\begin{pmatrix} \Delta(1/n^2)_1 \\ \Delta(1/n^2)_2 \\ \Delta(1/n^2)_3 \\ \Delta(1/n^2)_4 \\ \Delta(1/n^2)_5 \\ \Delta(1/n^2)_6 \end{pmatrix} = \begin{pmatrix} r_{11} & r_{12} & r_{13} \\ r_{21} & r_{22} & r_{23} \\ r_{31} & r_{32} & r_{33} \\ r_{41} & r_{42} & r_{43} \\ r_{51} & r_{52} & r_{53} \\ r_{61} & r_{62} & r_{63} \end{pmatrix} \begin{pmatrix} E_x \\ E_y \\ E_z \end{pmatrix}.$$
$$(5.4)$$

2

The coefficients r_{ij} are typically of the order 1 pm/V. The form of the r-matrix depends, as the second-order susceptibility or piezoelectric tensor, on crystal symmetry. The polarization as a result of mechanical forces can be described by

$$
\begin{pmatrix} P_x \\ P_y \\ P_z \end{pmatrix} = \begin{pmatrix} d_{11} & d_{12} & d_{13} & d_{14} & d_{15} & d_{16} \\ d_{21} & d_{22} & d_{23} & d_{24} & d_{25} & d_{26} \\ d_{31} & d_{32} & d_{33} & d_{34} & d_{35} & d_{36} \end{pmatrix} \begin{pmatrix} \sigma_{11} \\ \sigma_{22} \\ \sigma_{33} \\ \sigma_{23} \\ \sigma_{13} \\ \sigma_{13} \\ \sigma_{12} \end{pmatrix} .
$$

Here the σ_{ij} are the tensile, compressional, and shear stress, and the coefficients d_{ij} represent the piezoelectric tensor. Table 5.1 provides examples of the electro-optic coefficients of the 7 crystal systems.

Table 9.1. *The electro-optic $\bar{\bar{r}}$ for the 32 crystal symmetry classes.* · *zero element,* • *nonzero element,* •——• *equal nonzero elements,* •------o *equal nonzero elements of opposite sign. Centrosymmetric classes – all elements of $\bar{\bar{r}}$ are zero.*

Triclinic

$$\begin{pmatrix} \bullet & \bullet & \bullet \\ \bullet & \bullet & \bullet \\ \bullet & \bullet & \bullet \\ \bullet & \bullet & \bullet \\ \bullet & \bullet & \bullet \\ \bullet & \bullet & \bullet \end{pmatrix}$$

Example: Calcium thiosulphate ($CaS_2O_3.6H_2O$) strontium tartrate ($SrH_2(C_4H_4O_6)_2.4H_2O$)

Monoclinic

$$\begin{pmatrix} \cdot & \bullet & \cdot \\ \bullet & \cdot & \cdot \\ \cdot & \bullet & \cdot \\ \bullet & \cdot & \bullet \\ \cdot & \bullet & \cdot \\ \bullet & \bullet & \bullet \end{pmatrix}$$

2 (symmetry axis parallel to y)

$$\begin{pmatrix} \cdot & \cdot & \bullet \\ \cdot & \cdot & \bullet \\ \cdot & \cdot & \bullet \\ \bullet & \bullet & \cdot \\ \bullet & \bullet & \cdot \\ \cdot & \cdot & \bullet \end{pmatrix}$$

2 (symmetry axis parallel to z)

Examples: lithium sulphate ($LiSO_4.H_2O$), tartaric acid triglycine sulphate

$$\begin{pmatrix} \bullet & \cdot & \bullet \\ \bullet & \cdot & \bullet \\ \bullet & \cdot & \bullet \\ \cdot & \bullet & \cdot \\ \cdot & \bullet & \cdot \\ \cdot & \bullet & \cdot \end{pmatrix}$$

m (perpendicular to y)

$$\begin{pmatrix} \bullet & \bullet & \cdot \\ \bullet & \bullet & \cdot \\ \bullet & \bullet & \cdot \\ \cdot & \cdot & \bullet \\ \cdot & \cdot & \bullet \\ \bullet & \bullet & \cdot \end{pmatrix}$$

m (perpendicular to z)

Example: potassium nitrite (KNO_2)

Orthorhombic

$$\begin{pmatrix} \cdot & \cdot & \cdot \\ \cdot & \cdot & \cdot \\ \cdot & \cdot & \cdot \\ \bullet & \cdot & \cdot \\ \cdot & \bullet & \cdot \\ \cdot & \cdot & \bullet \end{pmatrix}$$

222

Examples: α–iodic acid (α–HIO_3), magnesium sulphate ($MgSO_4.7H_2O$), Rochelle salt ($KNaC_4H_4O_6.4H_2O$)

$$\begin{pmatrix} \cdot & \cdot & \bullet \\ \cdot & \cdot & \bullet \\ \cdot & \cdot & \bullet \\ \cdot & \bullet & \cdot \\ \bullet & \cdot & \cdot \\ \cdot & \cdot & \cdot \end{pmatrix}$$

mm2

Examples: Barium sodium niobate ($Ba_2NaNb_5O_{15}$), polyvinylidine fluoride (PVF), $(CH_2CF_2)_n$

Table 9.1. (cont.)

Tetragonal
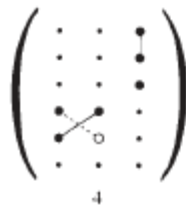
Example: iodo succinimide $(CH_2CO)_2NI$

4
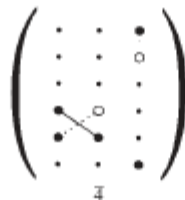
Examples: pentaerythritol $(C(CH_2OH)_4)$, cahnite $(Ca_4B_2As_2O_{12}.4H_2O)$

$\bar{4}$

Example: nickel sulphate $NiSO_4.6H_2O$

422

Example: $BaTiO_3$

4 mm

Examples: KDP, ADP, $CdGeAs_2$, $AgGaSe_2$, $AgGaS_2$

$\bar{4}2m$ (2-fold axis parallel to x)

Cubic

Examples: ($\bar{4}3m$): GaAs, InAs, GaP, ZnSe, CdTe, InSb. (23): Sodium chlorate ($NaClO_3$), sodium bromate ($NaBrO_3$)
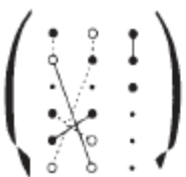
$\bar{4}3$ mm, 23

432
(lacks a center of symmetry, but other symmetry elements make all elements zero)

Trigonal

Example: sodium periodate $NaIO_4.3H_2O$

Examples: quartz, Te, mercury sulphide (α–HgS)
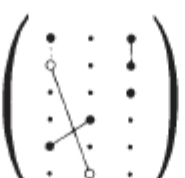
Examples: $LiNbO_3$, $LiTaO_3$, proustite (Ag_3AsS_3), pyrargyrite (Ag_3SbS_3)

3m (m perpendicular to x) standard orientation

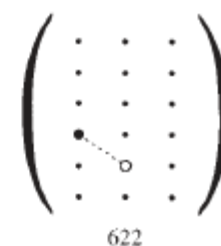3m (m perpendicular to y)

LiNbO$_3$ is THE crystal for EOMs

5

Table 9.1. (*cont.*)

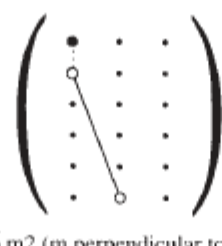Hexagonal
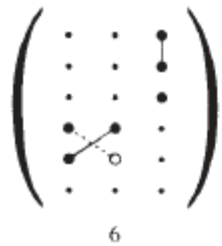
Examples:
lithium iodate
(LiIO$_3$),
Iodoform (CHI$_3$)

6

Examples:
CdS, CdSe,
ZnS, ZnO

6 mm

Examples:
barium
aluminate
(BaAl$_2$O$_4$)
kalsilite
(KAlSiO$_4$)

622

$\bar{6}$
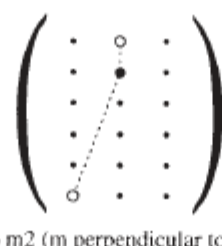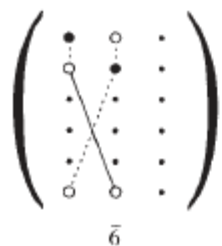
Examples:
benitoite (BaTiSi$_3$O$_9$)

$\bar{6}$ m2 (m perpendicular to x)
standard orientation

$\bar{6}$ m2 (m perpendicular to y)

6

For an applied field, the index ellipsoid changes according to

$$\left[\frac{1}{n_1^2} + \Delta\left(\frac{1}{n^2}\right)_1\right] x^2 + \left[\frac{1}{n_2^2} + \Delta\left(\frac{1}{n^2}\right)_2\right] y^2 + \left[\frac{1}{n_3^2} + \Delta\left(\frac{1}{n^2}\right)_3\right] z^2$$
$$+2\left[\frac{1}{n_4^2} + \Delta\left(\frac{1}{n^2}\right)_4\right] yz + 2\left[\frac{1}{n_5^2} + \Delta\left(\frac{1}{n^2}\right)_5\right] xz + 2\left[\frac{1}{n_6^2} + \Delta\left(\frac{1}{n^2}\right)_6\right] xy = 1,$$

(5.5)

If the crystal is oriented along the principle axes, it follows

$$\left[\frac{1}{n_1^2} + \Delta\left(\frac{1}{n^2}\right)_1\right] x^2 + \left[\frac{1}{n_2^2} + \Delta\left(\frac{1}{n^2}\right)_2\right] y^2 + \left[\frac{1}{n_3^2} + \Delta\left(\frac{1}{n^2}\right)_3\right] z^2$$
$$+2\Delta\left(\frac{1}{n^2}\right)_4 yz + 2\Delta\left(\frac{1}{n^2}\right)_5 xz + \Delta\left(\frac{1}{n^2}\right)_6 xy = 1.$$

(5.6)

It becomes immediately clear, that the linear electro-optic effect can only occur in non-centrosymmetric media, otherwise it would require

$$\Delta\left(\frac{1}{n^2}\right)_i = \sum_{j=1}^{3} r_{ij} E_j = -\sum_{j=1}^{3} r_{ij} E_j,$$

(5.7)

i.e., all coefficients would vanish. In general, changes in the index ellipsoid can

electric field generates also stress in a crystal due to the inverse piezo-electric effect. For low frequencies, the crystal displacements can follow the stress due to the electric field. For high frequencies that is not necessarily the case and therefore one has to expect that the coefficients for this process are different for low and high frequencies

$$r_{ij}^{dc} \neq r_{ij}^{hf}.$$

For an isotropic medium with photo-elastic effect, we have

$$\frac{1}{n^2} - \frac{1}{n_0^2} = pS, \tag{5.8}$$

or in short

$$\Delta n = \frac{n_0^3}{2} pS, \tag{5.9}$$

where p is the photo-elastic or elasto-optic coefficient, and S is the deformation. Eq. (5.9) is for example useful to describe the index change due to an acoustic wave. In the anisotropic case, the photo-elastic effect is described by

$$\Delta \left(\frac{1}{n^2} \right)_i = \sum_{k=1}^{6} \pi_{ik} \sigma_k, \tag{5.10}$$

where π_{ik} denotes the elasto-optic coefficients and σ_k the stress values.

5.1.1 Longitudinal electro-optic effect and modulators

To see how the electro-optic effect is used for the construction of modulators, we consider the case of potassium dihydrogen phosphate (KDP, KH_2PO_4). The related materials (KD*P, KD_2PO_4), ammonium dihydrogen phosphate (ADP, $(NH_4)(H_2PO_4)$) or (AD*P, $(NH_4)(D_2PO_4)$) behave similarly. These materials belong to the crystal class $\overline{4}2m$ and the electro-optic tensor has the form

$$\mathbf{r} = \begin{pmatrix} 0 & 0 & 0 \\ 0 & 0 & 0 \\ 0 & 0 & 0 \\ r_{41} & 0 & 0 \\ 0 & r_{41} & 0 \\ 0 & 0 & r_{63} \end{pmatrix}. \tag{5.11}$$

If we apply an electric field $\mathbf{E} = E_x\mathbf{e}_x + E_y\mathbf{e}_y + E_z\mathbf{e}_z$, we obtain for the index ellipsoid

$$\frac{x^2 + y^2}{n_0^2} + \frac{z^2}{n_e^2} + 2r_{41}E_xyz + 2r_{41}E_yxz + 2r_{63}E_zxy = 1. \tag{5.12}$$

If we have a field with only a z-component

$$\frac{x^2 + y^2}{n_0^2} + \frac{z^2}{n_e^2} + 2r_{63}E_z xy = 1. \qquad (5.13)$$

Since the equation is symmetric in x and y, the main axes are rotated by $45°$ against the x-y-coordinate system and z is invariant (see Fig. 5.1)

$$x = x'\cos 45° + y'\sin 45°, \qquad (5.14)$$
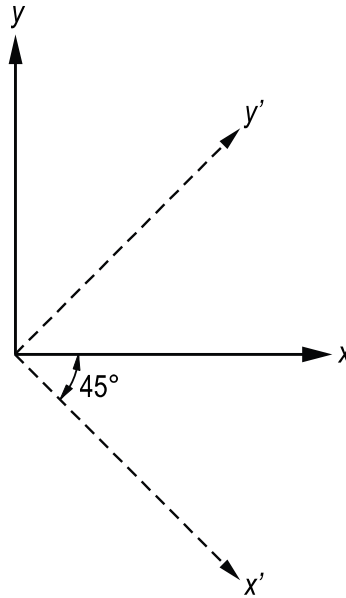$$y = -x'\sin 45° + y'\cos 45°. \qquad (5.15)$$

Figure 5.1: Rotation of the main axes for the $\bar{4}2m$ symmetry class for the case of an electric field applied in z-direction.

Substitution into Eq. (5.13) leads to

$$\left(\frac{1}{n_0^2} - r_{63}E_z\right) x'^2 + \left(\frac{1}{n_0^2} + r_{63}E_z\right) y'^2 + \frac{z^2}{n_e^2} = 1. \qquad (5.16)$$

Due to the applied field, the crystal becomes slightly biaxial and shows along the main axes the refractive indices

$$n^2 \qquad \frac{n_0^2}{} \qquad n^2 \qquad \frac{n_0^2}{} \qquad n^2 \qquad n^2 \qquad (5.17)$$

ctive index are small, i.e., $n_0^2 r_{63} E_z \ll 1$,

$$n_{x'} = n_0 \left(1 + \frac{1}{2} n_0^2 r_{63} E_z\right); \; n_{y'} = n_0 \left(1 - \frac{1}{2} n_0^2 r_{63} E_z\right); \; n_{z'} = n_e. \quad (5.18)$$

If a wave propagates inside the crystal in z-direction, the different polarizations experience a phase shift with respect to each other

$$\Delta\phi = \frac{2\pi L}{\lambda_0}\left(n_x' - n_y'\right) = \frac{2\pi L n_0^3 r_{63} E_z}{\lambda_0}. \tag{5.19}$$

The crystal thus acts as a voltage-dependent waveplate. The half-wave voltage, i.e., the voltage for a differential phase shift of π, is

$$V_\pi = \frac{\lambda_0}{2n_0^3 r_{63}}. \tag{5.20}$$

For KDP with $r_{63} = -10.5$ pm/V, $n_0 = 1.51$ at a wavelength of 632.8 nm, the half-wave voltage is $V_\pi = 8752$ V. If the input wave is rotated by 45° with respect to the x', y' axes, see Fig. 5.2, i.e., parallel to the x or y axis, then the half-wave plate turns the polarization by 90°. If the voltage is continuously increased to V_π, then the polarization evolves from initially linear to circular and finally again linear polarization, see Fig. 5.3. The polarization evolution can be used to construct a modulator.
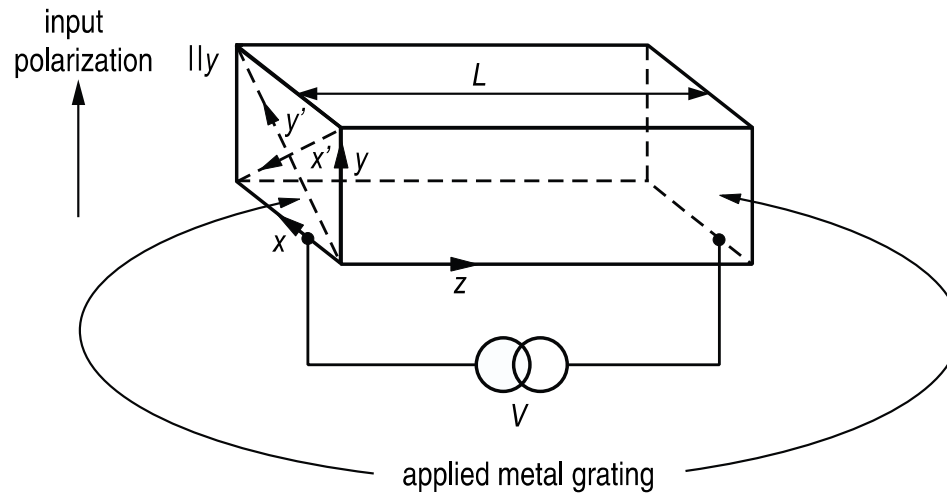
Needs electrodes on input and output facets

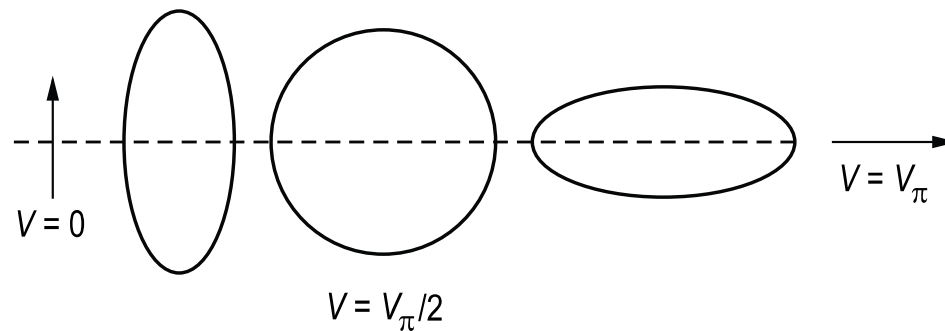Figure 5.2: KDP crystal orientation for a longitudinal electro-optic modulator.

Figure 5.3: Change in polarization state along propagation through the crystal due to the electro-optic phase retardation as shown in Fig. 5.2.

5.1.2 Transverse electro-optic effect and modulators

lithium niobate:

LiNbO$_3$

crystal class 3m

$$\mathbf{r} = \begin{pmatrix} 0 & -r_{22} & r_{13} \\ 0 & r_{22} & r_{13} \\ 0 & 0 & r_{33} \\ 0 & r_{51} & 0 \\ r_{51} & 0 & 0 \\ -r_{22} & 0 & 0 \end{pmatrix}.$$
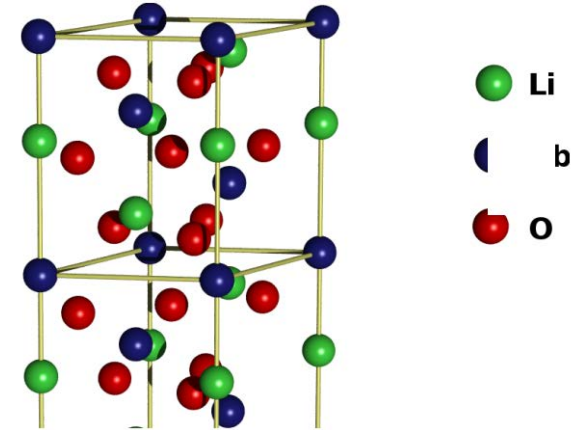
The index ellipsoid for the crystal without applied voltage has the form

$$\frac{x^2}{n_0^2} + \frac{y^2}{n_0^2} + \frac{z^2}{n_e^2} = 1. \tag{5.22}$$

With a field applied in y-direction, the index ellipsoid reads

$$\left(\frac{1}{n_0^2} - r_{22} E_y \right) x^2 + \left[\left(\frac{1}{n_0^2} + r_{22} E_y \right) y^2 + \frac{z^2}{n_e^2} + 2 r_{51} E_y yz \right] = 1. \tag{5.23}$$
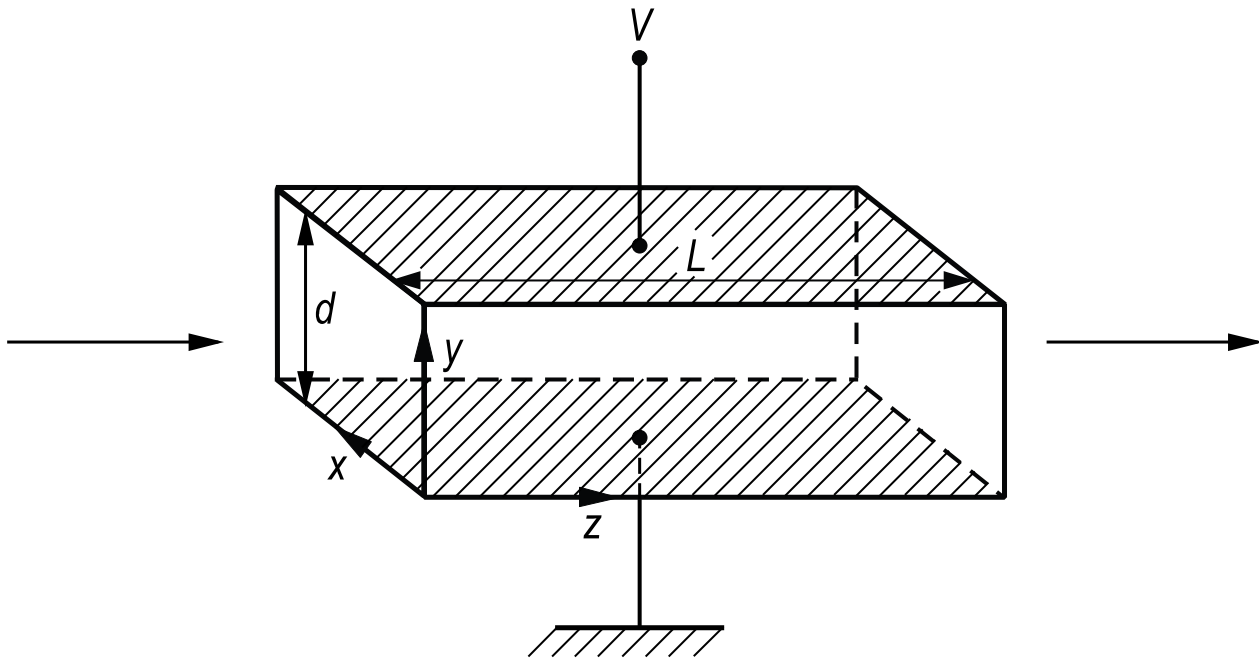
Figure 5.4: Orientation of a LiNbO$_3$ crystal to implement a transverse electro-optic modulator.
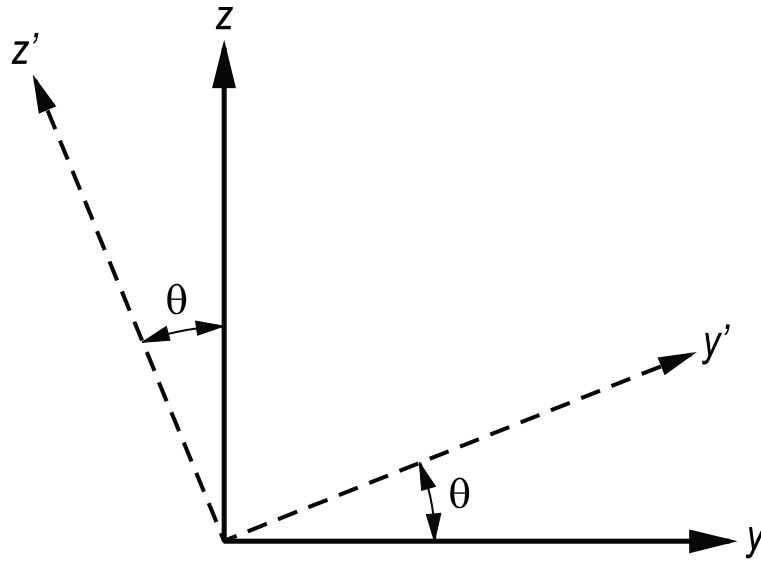
Figure 5.5: Rotation of the main axes in LiNbO$_3$, if an electric field is applied along the y-axis.

Because of the cross-term yz, the main axes are not preserved, and we transform to a new system, see Fig. 5.5, via

$$
\begin{aligned}
x &= x' \\
y &= y' \cos\theta - z' \sin\theta \\
z &= z' \cos\theta + y' \sin\theta.
\end{aligned}
\tag{5.24}
$$

The *x*-axis remains invariant and stays a main axis. Substitution into Eq. (5.23) leads to the following condition, that the cross-term vanishes

$$\left(\frac{1}{n_e^2} - \frac{1}{n_0^2} - r_{22}E_y\right)\sin\theta\cos\theta + r_{51}E_y(2\cos^2\theta - 1) = 0. \qquad (5.25)$$

Typically, the nonlinear coefficients are small and therefore also the necessary angle of rotation θ is small, i.e., $\theta \sim \sin\theta$ and $\cos\theta \sim 1$, and therefore θ simplifies to

$$\theta = \frac{-r_{51}E_y}{} \qquad (5.26)$$

Thus, the angle θ is really small. Since LiNbO$_3$ is a negative uniaxial crystal, i.e., $n_e < n_0$, the angle θ is negative. For the index ellipsoid in the new

$$\left(\tfrac{1}{n_0^2} - r_{22}E_y\right)x'^2 + \left[\left(\tfrac{1}{n_0^2} + r_{22}E_y\right)\cos^2\theta + \tfrac{\sin^2\theta}{n_e^2} + r_{51}E_y\sin 2\theta\right]y'^2$$
$$+ \left[\left(\tfrac{1}{n_0^2} + r_{22}E_y\right)\sin^2\theta + \tfrac{\cos^2\theta}{n_e^2} - r_{51}E_y\sin 2\theta\right]z'^2 = 1. \tag{5.27}$$

For $\theta \sim \sin\theta$ and $\cos\theta \sim 1$, we obtain

$$\left(\tfrac{1}{n_0^2} - r_{22}E_y\right)x'^2 + \left(\tfrac{1}{n_0^2} + r_{22}E_y + 2r_{51}E_y\theta + \tfrac{\theta^2}{n_e^2}\right)y'^2$$
$$+ \left[\left(\tfrac{1}{n_0^2} + r_{22}E_y\right)\theta^2 - 2r_{51}E_y\theta + \tfrac{1}{n_e^2}\right]z'^2 = 1. \tag{5.28}$$

So we read off for the indices of the main axes

$$
\begin{aligned}
\frac{1}{n_{x'}^2} &= \frac{1}{n_0^2} - r_{22}E_y, \\[2mm]
\frac{1}{n_{y'}^2} &= \frac{1}{n_0^2} + r_{22}E_y + 2r_{51}E_y\theta + \frac{\theta^2}{n_0^2}, \\[2mm]
\frac{1}{n_{z'}^2} &= \left(\frac{1}{n_0^2} + r_{22}E_y\right)\theta^2 - 2r_{51}E_y\theta + \frac{1}{n_e^2}.
\end{aligned}
\tag{5.29}
$$

Since θ is very small, we can neglect the terms proportional to θ

$$\frac{x^2}{n_x^2} + \frac{y^2}{n_y^2} + \frac{z^2}{n_z^2} = 1, \tag{5.30}$$

with

$$
\begin{aligned}
n_x &= \frac{n_0}{\sqrt{1 - n_0^2 r_{22} E_y}} = n_0 \left(1 + \frac{1}{2} n_0^2 r_{22} E_y\right), \\
n_y &= \frac{n_0}{\sqrt{1 + n_0^2 r_{22} E_y}} = n_0 \left(1 - \frac{1}{2} n_0^2 r_{22} E_y\right), \\
n_z &= n_{e.}
\end{aligned}
\tag{5.31}
$$

Again, if a wave propagates along the z-direction with polarization along the x- or y-direction, see Fig. 5.4, then the two polarizations pick up a differential phase shift

$$\Delta\phi = \frac{2\pi L}{\lambda_0} (n_x - n_y) = \frac{2\pi L n_o^3 r_{22} V}{\lambda_0 d} \tag{5.32}$$

and the corresponding half-wave voltage is

$$V_\pi = \frac{\lambda_0 d}{2 L n_0^3 r_{22}}. \tag{5.33}$$

For the values $d = 5$ mm, $L = 10$ mm, $n_o = 2.3$, $r_{22} = 3.4 \cdot 10^{-12}$ m/V at a wavelength of $\lambda_0 = 530$ nm, we observe the half-wave voltage $V_\pi = 1600$ V.

Another possibility to build a modulator from $LiNbO_3$ is given by the fact that a light wave propagates into y-direction and applying the field along the z-axis. The index ellipsoid then reads

$$\left(\frac{1}{n_0^2} + r_{13}E_z\right) x^2 + \left(\frac{1}{n_0^2} + r_{13}E_z\right) y^2 + \left(\frac{1}{n_e^2} + r_{33}E_z\right) z^2 = 1. \qquad (5.34)$$

In this case, the main axes remain

$$\frac{1}{n_0'^2} = \left(\frac{1}{n_0^2} + r_{13}E_z\right), \qquad (5.35)$$

$$\frac{1}{n_e'^2} = \left(\frac{1}{n_e^2} + r_{33}E_z\right).$$

With $r_{13}E_z \ll 1/n_0^2$ and $r_{33}E_z \ll 1/n_e^2$ we obtain the following refractive indices along the main axes

$$n_0' = \frac{n_0}{\sqrt{1 + r_{13}n_0^2 E_z}} = n_0\left(1 - \frac{1}{2}r_{13}n_0^2 E_z\right), \qquad (5.36)$$

$$n_e' = \frac{n_e}{\sqrt{1 + r_{33}n_e^2 E_z}} = n_e\left(1 - \frac{1}{2}r_{33}n_e^2 E_z\right).$$

With these expressions, we obtain for the differential phase shift between ordinary and extraordinary wave

$$\Delta\phi = \frac{2\pi L}{\lambda_0}\left(n_e' - n_0'\right), \tag{5.37}$$

$$\Delta\phi = \frac{2\pi L}{\lambda_0}\left[n_e - n_0 + \frac{1}{2}\left(r_{33}n_e^3 - r_{13}n_o^3\right)E_z\right]. \tag{5.38}$$

The half-wave voltage is then

$$V_\pi = \frac{\lambda_0 d}{L\left(r_{33}n_e^3 - r_{13}n_0^3\right)}. \tag{5.39}$$

With the values $d = 5$ mm, $L = 10$ mm, $r_{33}n_e^3 - r_{13}n_0^3 = 224$ pm/V at a wavelength of $\lambda_0 = 530$ nm, we obtain a half-wave voltage $V_\pi = 1183$ V. Despite the fact that this arrangement shows a lower half-wave voltage than the previous one evaluated by Eq. (5.33), it has a decisive disadvantage. The wave does not propagate along the optical axis, and therefore the crystal acts already as a waveplate even without an applied voltage. The field-independent

Birefringence compensation

phase shift $\Delta\phi_0 = \frac{2\pi L}{\lambda_0}(n_e - n_0)$ depends on temperature, which leads to a temperature-dependent bias. This problem can be mitigated by using two crossed crystals in sequence (o- and e- waves are exchanged in the second crystal, see Fig. 5.6), which cancels the field-independent bias. To avoid cancelation of the field-dependent effect, the field in the second crystal must be poled in reverse.
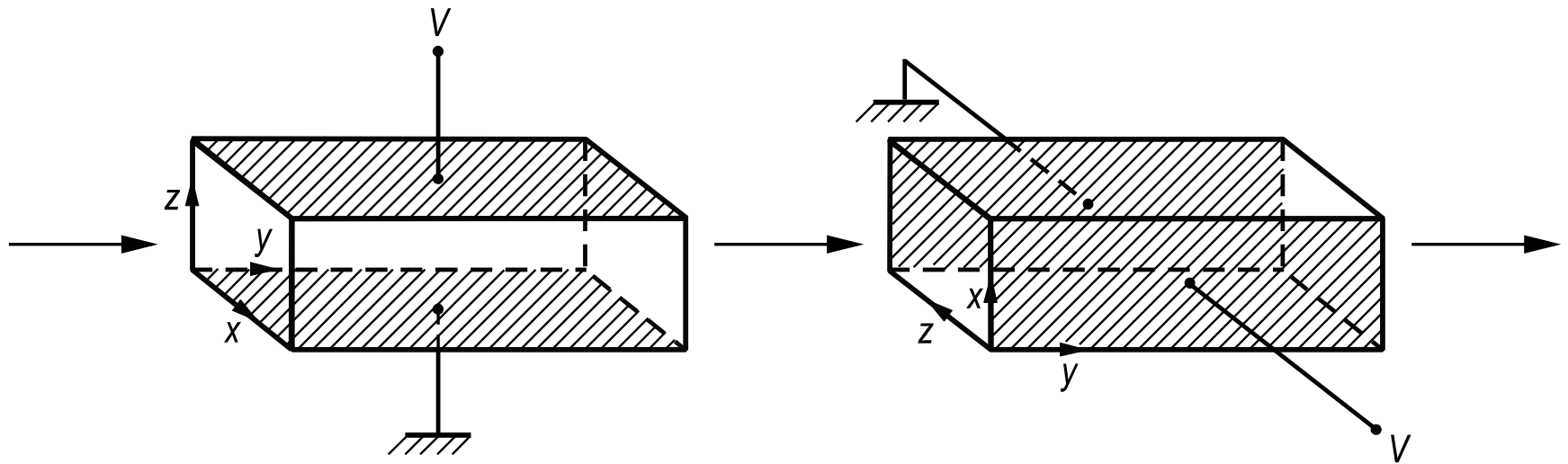

Figure 5.6: Transversal electro-optic modulator using two LiNbO$_3$ crystals rotated by 90° to compensate the field-independent birefringence.

5.2 Electro-optic amplitude modulator

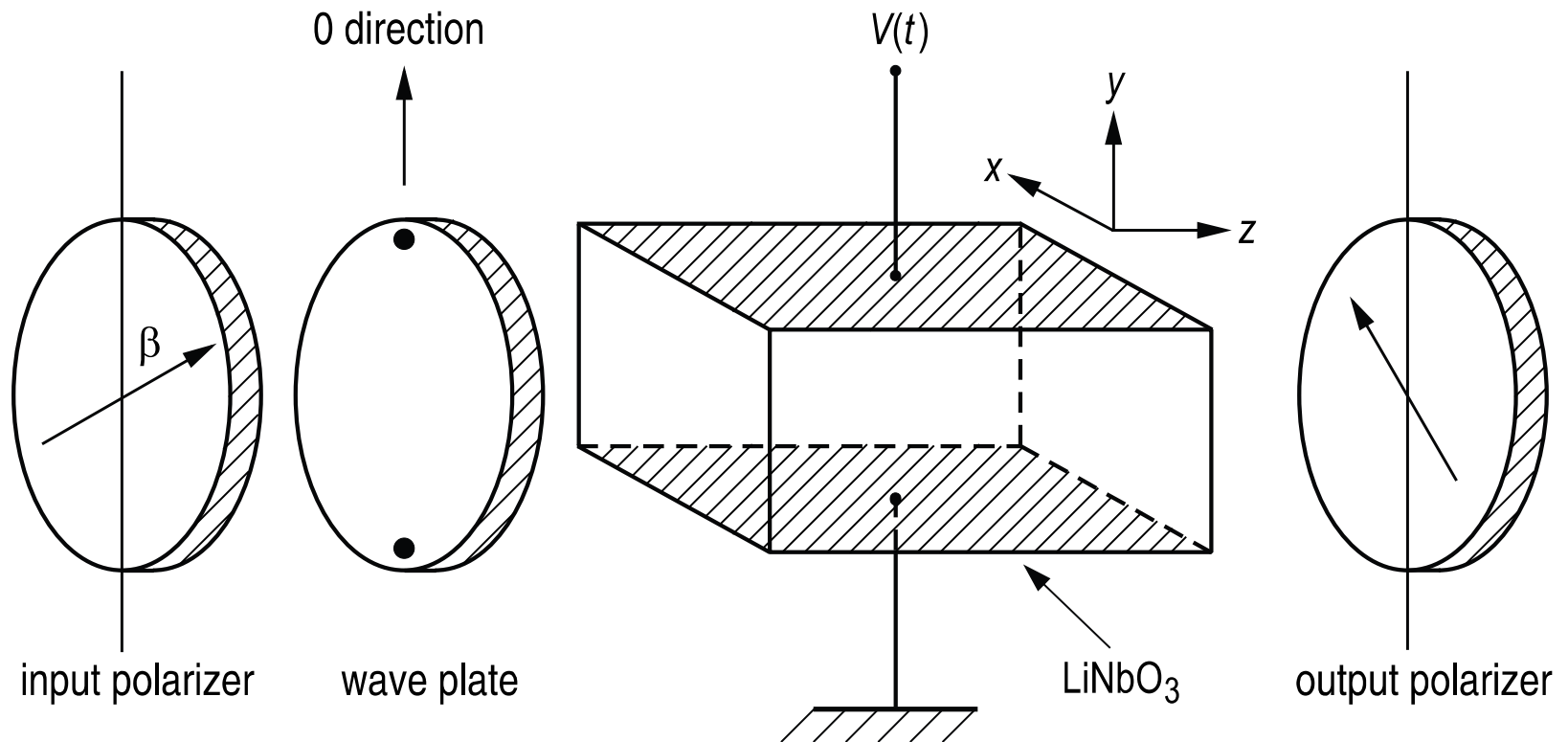**How is phase retardation converted into a amplitude modulation?**

Figure 5.7: Transversal electro-optic amplitude modulator from LiNbO$_3$.

Here, $\Delta\phi_{WP}$ is the phase retardation due to the field-independent birefrin-gence or due to an additional wave plate as shown in Fig. 5.7, and a is a co-efficient describing the relationship between field-dependent phase retardation and applied voltage. Usually we use $\beta = 45°$ to achieve 100 % transmission

$$\begin{aligned}\frac{I_{out}}{I_{in}} &= \frac{1}{2}\left\{1 - \cos\left[\Delta\phi_{WP} + aV\left(t\right)\right]\right\} &(5.43)\\ &= \frac{1}{2}\left\{1 - \cos\Delta\phi_{WP}\cos\left[aV\left(t\right)\right] + \sin\Delta\phi_{WP}\sin\left[aV\left(t\right)\right]\right\}.\end{aligned}$$

There are various applications for modulators. If the transmission through the modulator should be linearly dependent on the applied voltage, we use a bias $\Delta\phi_{WP} = \pi/2$ and obtain for $aV \ll 1$ (see also Fig. 5.8)

$$\frac{I_{out}}{I_{in}} = \frac{1}{2}\left\lceil 1 + aV\left(t\right)\right\rceil. \qquad (5.44)$$

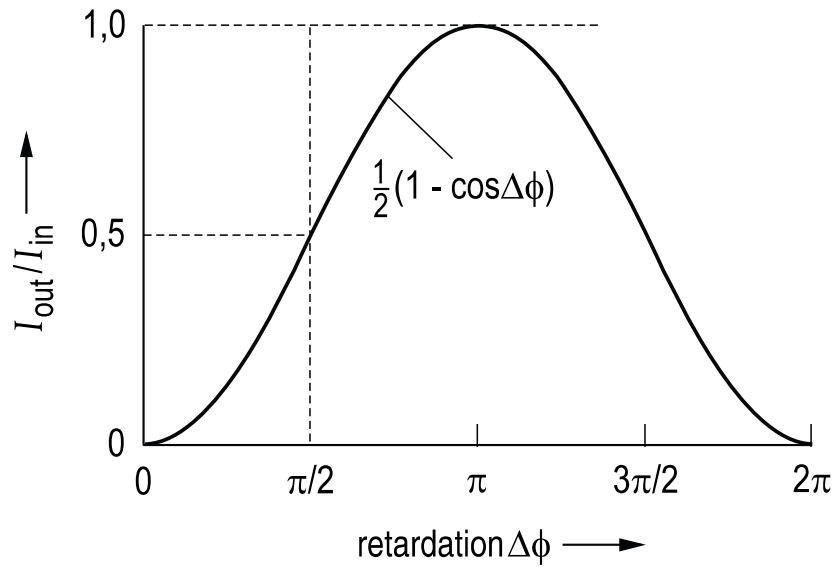$$\frac{{}_0 r_{22}}{\lambda_0 d}, \qquad (5.47)$$

Figure 5.8: Transmission characteristic of the modulator shown in Fig. 5.7 as a function of phase retardation.

where we used Eq. (5.33). With $\Delta\phi_{WP} = 0$, the relationship between output intensity and applied voltage is

$$\frac{I_{out}}{I_{in}} = \frac{1}{2}\left[1 - \cos\left(aV\left(t\right)\right)\right], \tag{5.48}$$

and, for small voltages $aV\left(t\right)$, we obtain a quadratic dependence

$$\frac{I_{out}}{I_{in}} = \frac{1}{4}a^2V^2\left(t\right). \tag{5.49}$$

5.3 Electro-optic phase modulator

$$\text{os}\left(\omega t + m \sin \omega_m t\right) \tag{5.52}$$
$$= \ E_0 \left[\cos \omega t \cos \left(m \sin \omega_m t\right) - \sin \omega t \sin \left(m \sin \omega_m t\right)\right],$$

with modulation depth m

$$m = \left(\frac{\pi n_0^3 r_{22}}{\lambda_0 d}\right) V_0. \tag{5.53}$$

With the generating functions for the Bessel functions

$$\cos\left(m \sin \omega_m t\right) = J_0\left(m\right) + 2 \sum_{k=1}^{\infty} J_{2k}\left(m\right) \cos\left(2k \omega_m t\right), \tag{5.54}$$

$$\sin\left(m \sin \omega_m t\right) = 2 \sum_{k=0}^{\infty} J_{2k+1}\left(m\right) \sin\left[\left(2k+1\right) \omega_m t\right], \tag{5.55}$$

and the addition theorem

$$2 \sin A \sin B = \cos\left(A - B\right) - \cos\left(A + B\right), \tag{5.56}$$

$$2 \cos A \cos B = \cos\left(A - B\right) + \cos\left(A + B\right), \tag{5.57}$$

the spectrum of the output field is

$$
\begin{aligned}
E_y^\omega\left(t\right) \quad = \quad & E_0 \left[J_0\left(m\right) \cos \omega t \right. \\
& + J_1\left(m\right) \cos\left(\omega + \omega_m\right) t - J_1\left(m\right) \cos\left(\omega - \omega_m\right) t \\
& + J_2\left(m\right) \cos\left(\omega + 2\omega_m\right) t + J_2\left(m\right) \cos\left(\omega - 2\omega_m\right) t \\
& + J_3\left(m\right) \cos\left(\omega + 3\omega_m\right) t - J_3\left(m\right) \cos\left(\omega - 3\omega_m\right) t
\end{aligned}
\tag{5.58}
$$

The spectrum consists of sidebands at multiples of the modulation frequency ω_m. An example is shown in Fig. 5.9.
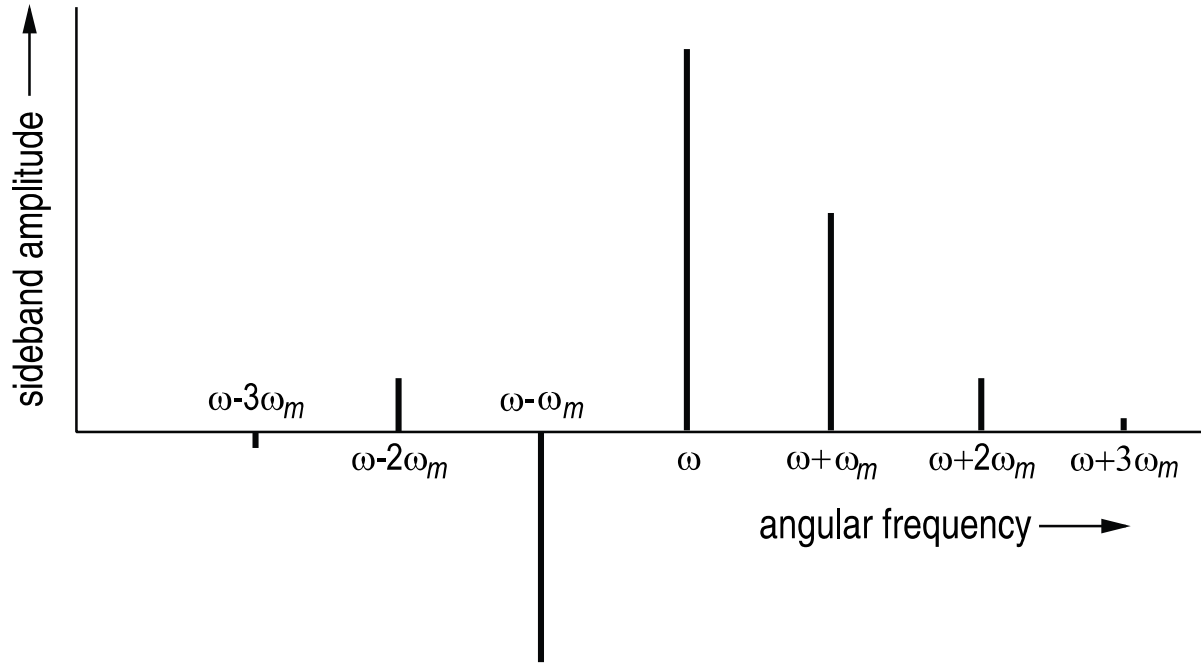

Figure 5.9: Phase-modulated spectrum with a modulation depth of $m = 1$.

5.4 Microwave modulator

High-speed or microwave signals are typically supplied by strip-lines or coplanar lines, see Eq. 5.10. For efficient modulation, the index modulation must copropagate in phase with the optical signal (group velocity, however, here we neglect dispersion, thus group velocity is equal to phase velocity).
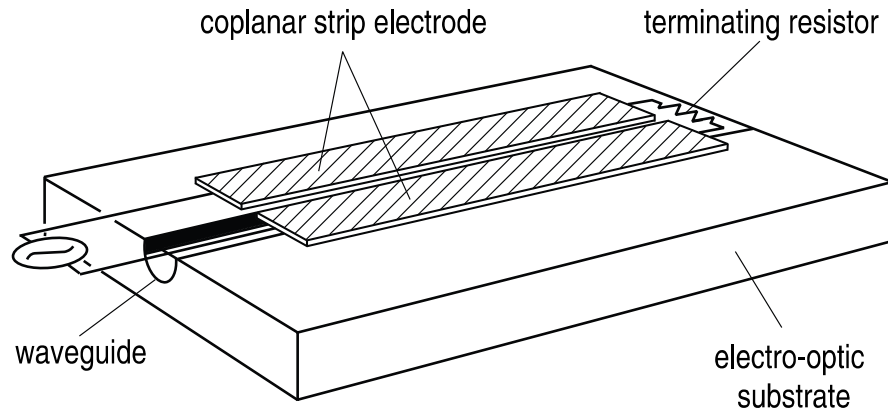

Figure 5.10: Electro-optic traveling wave modulator.

Let's assume the microwave signal

$$V(z,t) = V_0 \cos\left(\omega_m t - \frac{\omega_m n_m}{c_0} z\right), \qquad (5.59)$$

with phase velocity

$$c = \frac{c_0}{n_m}. \qquad (5.60)$$

If we consider the time slot of the optical wave that enters the crystal at $t = 0$, and copropagate with that time slot in the signal in the waveguide with effective index n, this time slot will experience the applied voltage

$$dz \tag{5.63}$$

$$= \frac{aV_0\omega}{c_0} \int_0^\ell \cos\left[\frac{\omega_m Z}{c_0}(n - n_m)\right] dz,$$

or

$$\Delta\phi = \frac{\omega a V_0}{\omega_m (n - n_m)} \sin\left[\frac{\omega_m \ell}{c_0} (n - n_m)\right].$$ (5.64)

As shown by Eq. (5.64), the phase modulation is the largest for arg=$\frac{\pi}{2}$, i.e.,

$$\frac{\omega_m \ell (n - n_m)}{c_0} = \frac{\pi}{2}; \text{ and } \omega_m = \omega_c.$$ (5.65)

which determines the optimum length of the modulator. For LiNbO$_3$, with $n_m = 4.2$, $n = 2.146$ and $\ell = 10$ mm, the maximum usable frequency is $\omega_c = 22.9$ GHz. The electric field acts on the waveguide as shown in Fig. 5.11. The waveguide can be fabricated, for example, by indiffusion of titanium. A buffer layer of Al$_2$O$_3$ or SiO$_2$ protects the optical field to interact with the metal electrodes to avoid losses. Typical data for a modulator are: waveguide width 7 μm, thickness of the buffer layer 260 nm, and thickness of the Cr/Au-electrodes is 3 μm. The index difference between core and cladding is about 0.01-0.02. Typical waveguide losses are 1 dB/cm at $\lambda = 633$ nm or 0.3 dB/cm for 1320 nm. The electro-optic tensor for LiNbO$_3$ is

$$\mathbf{r} = \begin{pmatrix} 0 & -3.4 & 8.6 \\ 0 & 3.4 & 8.6 \\ 0 & 0 & 30.8 \\ 0 & 28 & 0 \\ 28 & 0 & 0 \\ -3.4 & 0 & 0 \end{pmatrix} \times 10^{-13} \text{mV}^{-1}.$$ (5.66)

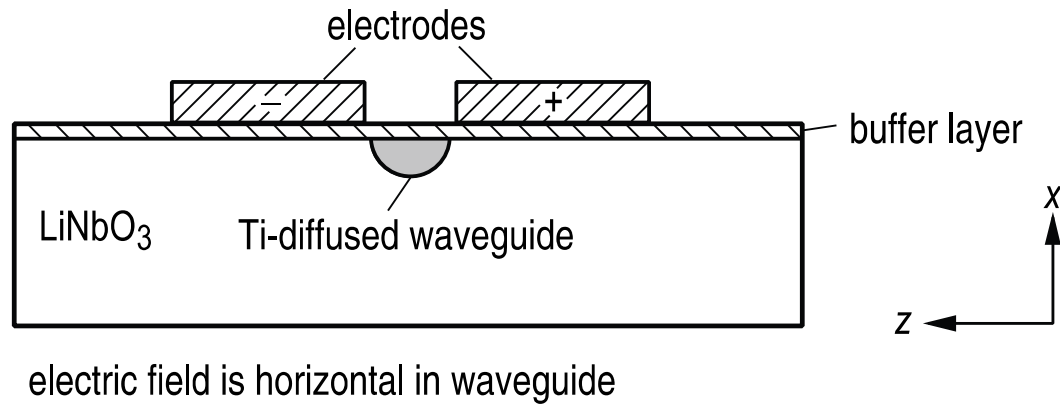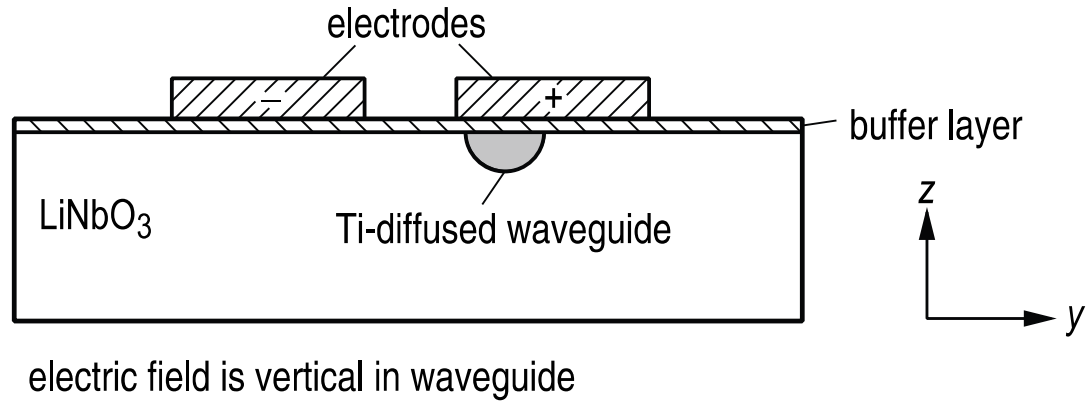electrodes

_   +

buffer layer

LiNbO$_3$ Ti-diffused waveguide

z

y

electric field is vertical in waveguide

electrodes

_   +

buffer layer

LiNbO$_3$ Ti-diffused waveguide

x

z

electric field is horizontal in waveguide

Figure 5.11: Geometry of a LiNbO$_3$ waveguide modulator: a) z-cut, TM mode b) x-cut, TE mode.